

Density functional theory study of $(\text{OCS})_2^-$

G. Bilalbegović

*Department of Physics, Faculty of Science, University of Zagreb, Bijenička 32,
10000 Zagreb, Croatia*

Abstract

The structural and electronic properties of the carbonyl sulfide dimer anion are calculated using density functional theory within a pseudopotential method. Three geometries are optimized and investigated: C_{2v} and C_2 symmetric, as well as one asymmetric structure. A distribution of an excess charge in three isomers are studied by the Hirshfeld method. In an asymmetric $(\text{OCS})_2^-$ isomer the charge is not equally divided between the two moieties, but it is distributed as $\text{OCS}^{-0.6}$. $\text{OCS}^{-0.4}$. Low-lying excitation levels of three isomers are compared using the time-dependent density functional theory in the Casida approach.

1 Introduction

Ionic nanoparticles of various sizes offer possibilities to investigate the change of a chemical bonding from molecules and clusters to the bulk. Studies of ionic clusters are important for understanding of microscopic aspects of chemical reactions in controlled environments [1]. Carbonyl sulfide may play an important role in an explanation of the origin of life on Earth. It acts as a condensing agent in the formation of peptides from amino acids [2]. This material is known as a component of volcanic gases and it is present in the atmosphere of Earth where it is a part of the global sulfur cycle. Carbonyl sulfide is also present in the atmosphere of Venus and in many other astrophysical objects. Therefore, OCS and related ions and clusters are important for various chemical and physical processes. It has been found that OCS^- anion is metastable, but that an addition of OCS or H_2O molecules produces a stable structure [3,4].

For homogeneous anionic clusters, such as $(\text{OCS})_n^-$, it is important to find out whether an excess electron is located in a vicinity of a particular monomer, or it is shared between two or more fragments. The photodissociation dynamics of $(\text{OCS})_2^-$ has been studied in the ion beam apparatus using a tandem time-of-flight mass spectrometry [5]. The photoelectron imaging method has been also

applied in the studies of $(\text{OCS})_2^-$ [3,6]. The coexistence of two covalent OCS_2^- isomers (having C_{2v} and C_2 symmetry), as well as electrostatically bound $\text{OCS}^- \cdot \text{OCS}$ have been proposed [1,5]. The formation of $(\text{OCS})_n^-$ cluster ions have been studied using low-energy electron attachment to molecular clusters $(\text{OCS})_n$ seeded in helium carrier gas [7]. This experiment have been supported by the coupled cluster theory calculations of electron affinity and vertical detachment energy of the carbonyl sulfide [7].

Advanced experimental methods, such as photoelectron spectroscopy, are able to explore various nanostructures. It is important to compare these results with different theoretical simulations of the same systems. The properties of $(\text{OCS})_2^-$ cluster have been studied using the Gaussian quantum chemistry code in connection with the photodissociation experiments [5]. A related $(\text{OCS})_2^+$ complex has also been investigated using the Gaussian program [8]. The pseudopotential based density functional theory is characterized by the computational efficiency and recent intensive developments. It is nowadays possible to use this method for big systems which exhibit complex chemical and physical processes. It allows computations of larger systems than traditional quantum chemistry methods. The pseudopotential time-dependent density functional theory is promising and still in development for many applications, for example in studies of charge transfer processes. It is important to use density functional theory and pseudopotentials to simulate some of the structures and processes studied in experiments on time-resolved dynamics and solvation in big anion clusters [1]. However, methods initially developed in theoretical chemistry sometimes better describe dynamics of electrons involved in chemical processes. Therefore, it is important to test the pseudopotential density functional methods in studies on small charged clusters. In the previous computational study of $(\text{OCS})_2^-$, which has been done using the Gaussian package [1,5], the charge population has not been analyzed, and a direct calculation of low-lying excited energy levels of different isomers has not been presented. In this work $(\text{OCS})_2^-$ is studied using density functional theory (DFT) electronic structure calculations. Three geometries of the carbonyl sulfide dimer anion are minimized and their structures, energies, the ground state electronic properties, as well as distributions of the lowest excitation levels are investigated.

2 Computational Method

DFT based calculations have been recently used as a powerful method for studies of bulk, surfaces, and nanostructures of various materials [9]. The structural and electronic properties of $(\text{OCS})_2^-$ are studied in this work using the plane wave density functional Abinit code [10]. This code is robust, accurate and widely used. It has been applied by many users on various geometries and processes, and it is therefore well tested. The local density approximation of

the exchange functional in the parametrization of Perdew and Wang is applied [11]. The $(\text{OCS})_2^-$ ions (and related structures used for testing and comparison) are positioned in the middle of the periodically replicated simulation box. The side of the box for most simulations was 30 a.u. The Brillouin zone is sampled using the Γ point. Relaxation of ions is carried out by performing a series of self-consistent calculations. The Broyden-Fletcher-Goldfarb-Shanno minimization method is used for a structural optimization and all atoms are allowed to move.

In the Abinit package charged systems are immersed in a neutralizing jellium background. For such charged particles artificial electrostatic interactions between the initial system and its periodic images in the supercells are possible [12,13,14]. However, the supercells used here are sufficiently large to avoid these effects. To check this point several calculations for larger cells (35 and 40 a.u.) are done and the differences in the total energy, bond lengths and angles are found to be 0.1% at the most. In addition, the charge density plots do not change when the side of the cell increases.

Because of a fragility of some possible $(\text{OCS})_2^-$ structures, two kinds of pseudopotentials are used and the results are compared. First, the calculations are carried out using the Troullier-Martins (TM) pseudopotentials [15], prepared by the Fritz Haber Institute code [16] and taken from the Abinit web page [10]. The cutoff of 35 Ha is used for the TM pseudopotentials. Calculations are also done using the relativistic separable pseudopotentials in the form of Hartwigsen, Goedecker and Hutter (HGH) [17]. The cutoff of 50 Ha is applied for the HGH pseudopotentials. It has been found that the properties of CS, CS_2 and several oxide molecules calculated using these pseudopotentials agree with experiments [17]. It is calculated in this work that both kinds of pseudopotentials (HGH and TM) produce a good agreement with experiments for the properties of OCS. This molecule (in experiments, as well as in calculations described here) stabilizes into a linear structure. The S-C distance is 1.548 Å (the experimental value is 1.561 Å [4]), and the C-O distance is 1.160 Å (the experimental result is 1.156 Å) in the calculations using the HGH pseudopotentials. The calculated distances are 1.548 Å and 1.148 Å, respectively for the S-C and C-O bonds, when the TM pseudopotentials are applied. For the $(\text{OCS})_2^-$ isomers, only small numerical differences are found between calculations carried out using the TM and HGH pseudopotentials. It is important to report the result for an electron affinity of the OCS molecule. However, it is not possible to stabilize $(\text{OCS})^-$ structure within the method used in this work and this is a necessary step for the calculation of electron affinity. The absence of a stable $(\text{OCS})^-$ anion in this calculation is in agreement with the experimental results. This anion is not formed in a standard ion source and almost no $(\text{OCS})^-$ is detected in the mass-spectrum [1,3,4,5,6].

The excitation energies are calculated within the time-dependent local density

Fig. 1. The density functional optimized structures and distances of symmetric $(\text{OCS})_2^-$: (a) C_{2v} , (b) C_2 . Bond lengths (in Ångströms) and angles (in degrees) are shown.

functional theory using the Casida approach [18,19] implemented in the Abinit code. In this method the time-dependent density functional theory (TDDFT) equations are studied in the frequency domain. The eigenvalue problem is solved for the matrix whose main part is formed of the squares of differences between occupied and unoccupied Kohn-Sham electronic energies. The coupling matrix which includes the contribution of the Coulomb and exchange-correlation interactions is also added to the Casida matrix. It is known that low-lying excited states of small, chemically simple clusters and molecules are well represented in the Casida approach. New algorithms in TDDFT are necessary for periodic systems and high-lying excited levels. In this work the Casida approach to TDDFT is used to compare low-lying excitation energy levels of three $(\text{OCS})_2^-$ isomers.

3 Results and discussion

Three equilibrium structures of $(\text{OCS})_2^-$ are stabilized within approximations of density functional theory used in this work and for both kinds of pseudopotentials. These calculations started from initial geometries close to those proposed by Sanov and coworkers [1,5]. Several other initial structures of $(\text{OCS})_2^-$ were also considered, but none of them is found to be stable. The equilibrium structures of $(\text{OCS})_2^-$, as well as corresponding bond lengths and angles calculated using the TM pseudopotentials are shown in Figs. 1 and 2. In the asymmetric $(\text{OCS})_2^-$ structure (shown in Fig. 2) both OCS fragments are non-linear. This also applies for the same isomer optimized using the HGH pseudopotentials. The electron charge isosurface plot for the asymmetric $(\text{OCS})_2^-$ structure is also shown in Fig. 2. Two moieties are bonded between the carbon atom of one fragment and the sulphur atom of the other. The distance between these two atoms is 2.49 Å. Figures 2 and 3(c) show that a weak covalent interaction between the two moieties exists. In the structures found by Sanov and coworkers one isomer is asymmetric. This is an electrostatically bound structure where one of the moieties is linear, and the charges are distributed as $\text{OCS}^- \cdots \text{OCS}$ [1,5]. Both asymmetric isomers, weakly covalent and electrostatically bonded one, may form under experimental conditions. The binding energies are presented in Table 1. The C_{2v} structure is the most stable. The differences in energy of about $\Delta E_1 = 0.25$ eV and $\Delta E_2 = 0.61$ eV exist between the C_{2v} structure and two other isomers. These results also show that the binding energy of the most stable structure of the C_{2v} $(\text{OCS})_2^-$ isomer is ~ 3 eV lower than one of the neutral C_{2v} $(\text{OCS})_2$ cluster optimized by the

Fig. 2. The density functional optimized asymmetric $(\text{OCS})_2^-$ structure. The electron charge density, as well as bond lengths (in Angströms) and angles (in degrees) are shown. The charge contour corresponds to a constant density equal to $0.02 \text{ eV}/a_0^3$.

Table 1

Binding energies (in eV) of three optimized anions of $(\text{OCS})_2^-$ and a neutral $(\text{OCS})_2$ cluster (having C_{2v} symmetry) calculated using the TM and HGH pseudopotentials.

Structure	$C_{2v} (\text{OCS})_2^-$	$C_2 (\text{OCS})_2^-$	asymmetrical $(\text{OCS})_2^-$	$(\text{OCS})_2$
TM	-46.794	-46.544	-46.188	-43.750
HGH	-46.602	-46.357	-46.002	-43.293

Fig. 3. The HOMO states of $(\text{OCS})_2^-$ isomers: (a) C_{2v} symmetric, (b) C_2 symmetric, (c) asymmetric structure. The light (dark) isosurface corresponds to the negative (positive) part of the wave functions.

same method.

The Hirshfeld method is a suitable technique to analyze the charge density distribution in molecules decomposed into atomic fragments [20,21]. In this method a molecule is divided into atomic contributions proportional to the weight of the free atom charge density. The free atoms situated in their corresponding positions in the molecule define the promolecule. This reference state of the promolecule is compared to the actual charge on the real molecule induced by the formation of chemical bonds. The Hirshfeld charges of $(\text{OCS})_2^-$ are shown in Tables 2 and 3. The third structure (the results shown in Table 3) is not symmetric and charges are different for two atoms in three pairs of the same kind (S, C, and O). A small positive charge is located on the carbon atoms in C_{2v} and C_2 symmetric structures, whereas a negative charge is distributed on all atoms in asymmetric $(\text{OCS})_2^-$. The results for the neutral $(\text{OCS})_2$ dimer (also presented in Table 2) show that charges on all atoms become more negative in $(\text{OCS})_2^-$. The oxygen Hirshfeld charges in $(\text{OCS})_2^-$ isomers are substantially lower than in the water molecule and in the carbonyl oxygen of the acetamide, but it is also higher than in the carbonyl oxygen of the formaldehyde [22]. These Hirshfeld charges for various molecules are calculated within different *ab initio* computational programs. However, previous calculations (for a different material) have been shown that the values of Hirshfeld charges are not sensitive to the calculation technique [23]. Table 3 shows that the excess charge in an asymmetric $(\text{OCS})_2^-$ structure is distributed as $-0.6 : -0.4$. More bended fragment of this isomer takes more, but not all of the negative charge. The part of the excess charge is located on the other moiety which is also bended.

Figure 3 presents the HOMO wave functions, whereas Fig. 4 shows the energy

Table 2

Hirshfeld charges of $(\text{OCS})_2^-$ for two symmetric structures calculated using the TM pseudopotentials. The charges on atoms in the C_{2v} symmetric neutral $(\text{OCS})_2$ cluster are also shown. The values for the HGH pseudopotentials are in the parenthesis.

Structure	$\text{C}_{2v} (\text{OCS})_2^-$	$\text{C}_2 (\text{OCS})_2^-$	$\text{C}_{2v} (\text{OCS})_2$
$\delta\text{Q}(\text{S})$	-0.251 (-0.250)	-0.296 (-0.294)	+0.049 (+0.049)
$\delta\text{Q}(\text{C})$	+0.026 (+0.018)	+0.038 (+0.030)	+0.100 (+0.092)
$\delta\text{Q}(\text{O})$	-0.274 (-0.268)	-0.241 (-0.235)	-0.149 (-0.141)

Table 3

Hirshfeld charges for the asymmetric $(\text{OCS})_2^-$ structure calculated using the TM pseudopotentials (the values for the HGH pseudopotentials are in the parenthesis). Atoms labeled with “1” belong to the moiety on the right in Fig. 2.

Structure	Atom 1	Atom 2
$\delta\text{Q}(\text{S})$	-0.156 (-0.154)	-0.344 (-0.343)
$\delta\text{Q}(\text{C})$	-0.006 (-0.016)	-0.010 (-0.016)
$\delta\text{Q}(\text{O})$	-0.232 (-0.226)	-0.245 (-0.238)

levels of optimized $(\text{OCS})_2^-$ isomers. Delocalized negative orbitals exist only in the C_2 symmetric (Fig. 3 (b)) and asymmetric structure (Fig. 3(c)). The σ -like bonding orbital exists between the carbon atom on the left fragment and the sulphur atom on the right one in the asymmetric structure (Fig. 3(c)). The details of electronic structure, such as a distribution of levels and shapes of HOMO states, are different for these three isomers. As in many other systems, these results show that the chemical and physical properties of nanostructures are determined not only by their size and the atoms they consist of. The details of geometrical and electronic structure are also important.

In experimental studies of $(\text{OCS})_2^-$ [3,5,6] it has been found that covalent isomers and asymmetric electrostatically bound $\text{OCS}^- \cdot \text{OCS}$ structure behave differently in photoexcitation. The availability of low-lying excited states has been suggested to explain the autodetachment electron emission from the covalently bound isomers. The results in Fig. 5 show that the most pronounced low excited levels exist for the C_2 symmetric isomers. The low-lying excited states do not appear in the asymmetric $(\text{OCS})_2^-$ structure. Therefore, this calculations shows that the C_2 covalently bound isomers are the most suitable for the autodetachment mechanism of electron emission.

In summary, three electronic isomers of the carbonyl sulfide dimer anion are stabilized and investigated using the pseudopotential based DFT computational methods. These three isomers of $(\text{OCS})_2^-$ have different geometrical and electronic properties, and therefore their participation in various chemical and physical processes is different. In particular, the Hirshfeld method

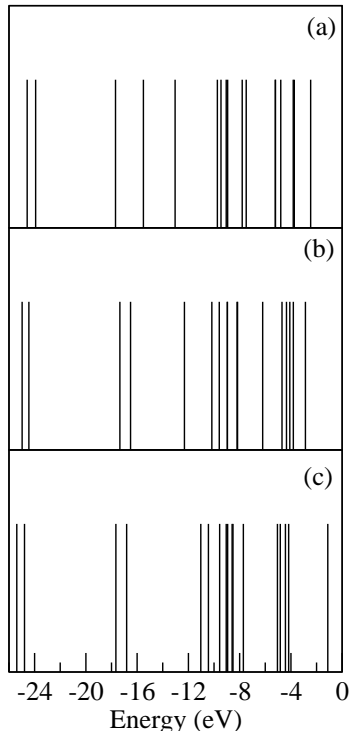


Fig. 4. Electron eigenvalues for $(\text{OCS})_2^-$ isomers: (a) C_{2v} symmetric, (b) C_2 symmetric, (c) asymmetric structure. Several levels are degenerate and almost degenerate, and therefore they are not distinguishable in the figure.

calculations show that a distribution of a negative charge strongly depends on the structure and that in an asymmetric isomer the charge is distributed as $-0.6 : -0.4$, where the more bended moiety takes more charge. The low-lying excited levels of $(\text{OCS})_2^-$ isomers are calculated within the time-dependent density functional method and the lowest excitations are found for the C_2 symmetric structure. This work describes three possible structures of the carbonyl sulfide dimer anion. These results are in rather good agreement with the previous computational results obtained by different method [1,5]. Two similar covalent isomers are obtained, but electrostatically bound $\text{OCS}^- \cdot \text{OCS}$ structure is not found in the present study. Instead weak covalent $\text{OCS}^{-0.6}$. $\text{OCS}^{-0.4}$ asymmetric structure is minimized. Many isomers, stable and metastable ones, may form under experimental conditions. Therefore, the existence of all four isomers are possible in experiments, and all of them may contribute to the time-resolved dynamics and solvation processes in $(\text{OCS})_n^-$ clusters. It is possible to assess the reliability of these calculations by comparison with the results of the Gaussian code [1,5]. The two lowest energy covalent isomers of the same symmetry are found using both methods and their computationally optimized structural parameters are close; the largest differences are below 2%. This agreement shows the precision and the reliability of both techniques, as well as the strengths of all modern computational methods in the studies of materials. The details of the structure and charge distribution in isomers

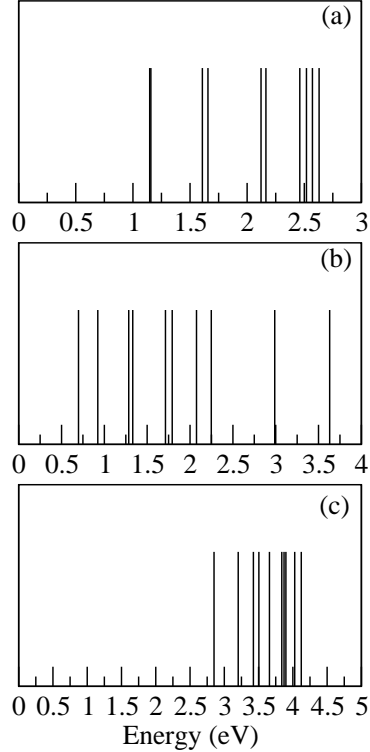


Fig. 5. The lowest excitation energies from the ground-state of $(\text{OCS})_2^-$ isomers: (a) C_{2v} symmetric, (b) C_2 symmetric, (c) asymmetric structure. The first ten mixed singlet and triplet energy levels are shown (several levels are not distinguishable on these figures).

of $(\text{OCS})_2^-$ are also important on a more general level because they play a role as a prototype for the $(\text{OCS})_n^-$ cluster ions and corresponding solvation effects. Because of the computational efficiency of the pseudopotential density functional theory method, it is possible to extend these calculations to larger anion clusters, such as $(\text{OCS})_n^-$ already studied in experiments described in Refs. [1,3,5]. The pseudopotential time-dependent density functional techniques, used in this work to compare distributions of low-lying excited energy levels, are now under intensive development. These methods should be useful in an interpretation of experimental results on the time-resolved dynamics of cluster anions and other nanostructures.

Acknowledgements

This work has been supported by the HR-MZOS projects “Dynamical Properties and Spectroscopy of Surfaces and Nanostructures” and “Electronic Properties of Surfaces and Nanostructures”. The visualizations were done using the XCrySDen package [24]. I would like to thank the University Computing Center SRCE for their support and computer time.

References

- [1] A. Sanov, W. C. Lineberger, *Phys. Chem. Comm.* **5** (2002) 165.
- [2] L. Leman, L. Orgel, M. R. Ghadiri, *Science* **306** (2004) 283.
- [3] E. Surber, A. Sanov, *J. Chem. Phys.* **118** (2003) 9192.
- [4] E. Surber, S. P. Ananthavel, A. Sanov, *J. Chem. Phys.* **116** (2002) 1920.
- [5] A. Sanov, S. Nandi, K. D. Jordan, W. C. Lineberger, *J. Chem. Phys.* **109** (1998) 1264.
- [6] E. Surber, A. Sanov, *Phys. Rev. Lett.* **90** (2003) 093001.
- [7] S. Barsotti, T. Sommerfeld, M. W. Ruf, H. Hotop, *Int. J. Mass Spectrom.* **233** (2004) 181.
- [8] M. L. McKee, *Chem. Phys. Lett.* **179** (1991) 559.
- [9] R. M. Martin, *Electronic Structure*, Cambridge University Press, Cambridge (2004).
- [10] X. Gonze, J. M. Beuken, R. Caracas, F. Detraux, M. Fuchs, G. M. Rignanese, L. Sindic, M. Verstraete, G. Zerah, F. Jollet, M. Torrent, A. Roy, M. Mikami, Ph. Ghosez, J. Y. Raty, D. C. Allan, *Comput. Mat. Sci.* **25** (2002) 478; <http://www.abinit.org>
- [11] J. P. Perdew, Y. Wang, *Phys. Rev. B* **45** (1992) 13244.
- [12] Y. Bar-Yam, J. D. Joannopoulos, *Phys. Rev. B* **30** (1984) 1844.
- [13] G. Makov, M. C. Payne, *Phys. Rev. B* **51** (1995) 4014.
- [14] P. A. Schultz, *Phys. Rev. B* **60** (1999) 1551.
- [15] N. Troullier, J. L. Martins, *Phys. Rev. B* **43** (1991) 1993.
- [16] M. Fuchs, M. Scheffler, *Comput. Phys. Commun.* **119** (1999) 67.
- [17] C. Hartwigsen, S. Goedecker, J. Hutter, *Phys. Rev. B* **58** (1998) 3641.
- [18] E. Runge, E. K. U. Gross, *Phys. Rev. Lett.* **52** (1984) 997.
- [19] M. E. Casida, in: D. P. Chong (Ed.), *Recent Advances in Density-Functional Methods, Part I*, World Scientific, Singapore, 1995, p. 155.
- [20] F. L. Hirshfeld, *Theoret. Chim. Acta* **44** (1977) 129.
- [21] R. F. Nalewajski, R. G. Parr, *J. Phys. Chem. A* **105** (2001) 7391.
- [22] F. De Proft, C. Van Alsenoy, A. Peeters, W. Langenaeker, P. Geerlings, *J. Comput. Chem.* **23** (2002) 1198.
- [23] G. Bilalbegović, *J. Phys.: Condens. Mat.* **18** (2006) 3829.
- [24] A. Kokalj, *Comput. Materials Sci.* **28** (2003) 155; Code available from <http://www.xcrysden.org>

This figure "Fig1.jpg" is available in "jpg" format from:

<http://arxiv.org/ps/0705.2159v1>

This figure "Fig2.jpg" is available in "jpg" format from:

<http://arxiv.org/ps/0705.2159v1>

This figure "Fig3.jpg" is available in "jpg" format from:

<http://arxiv.org/ps/0705.2159v1>